

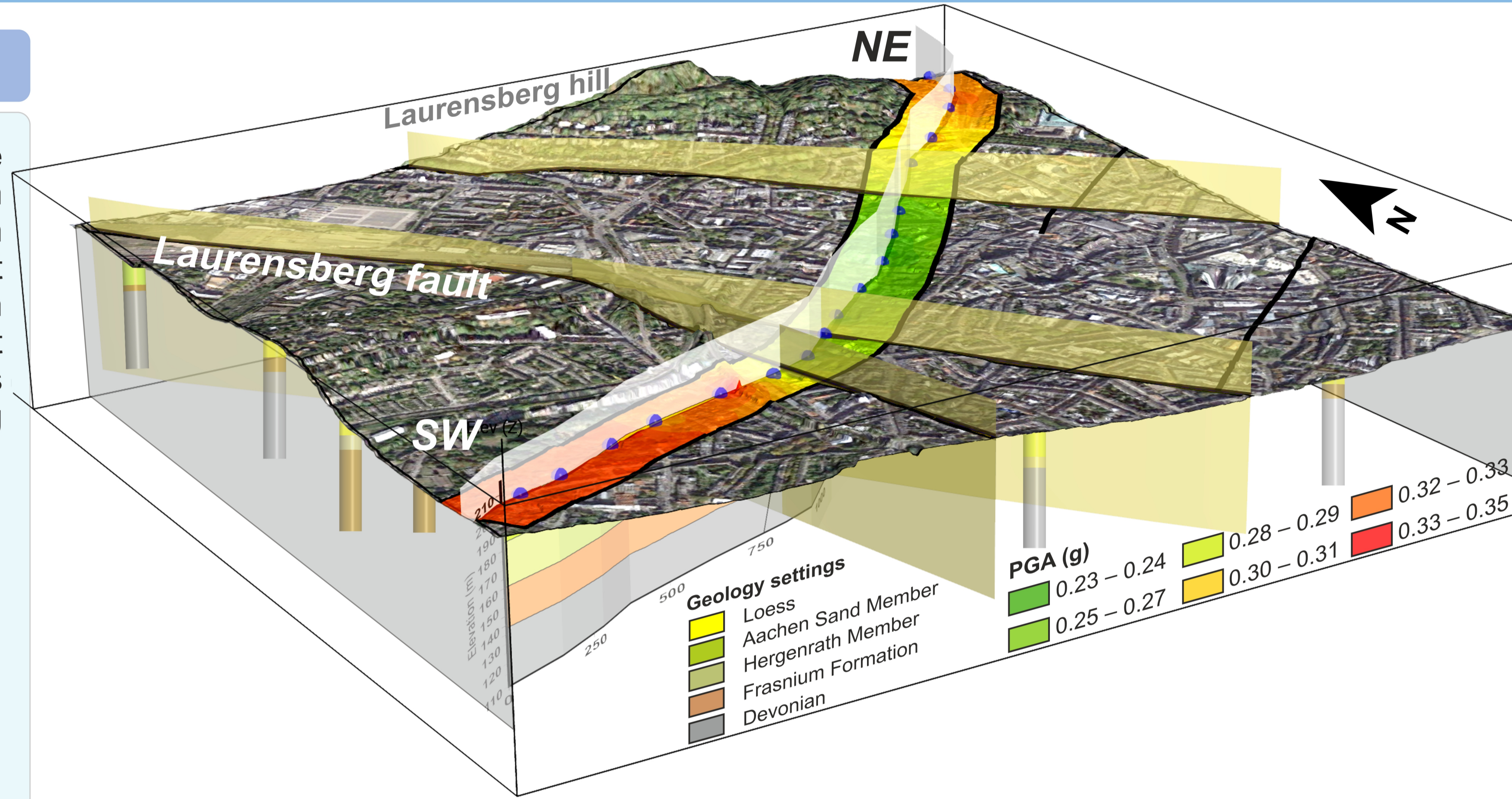
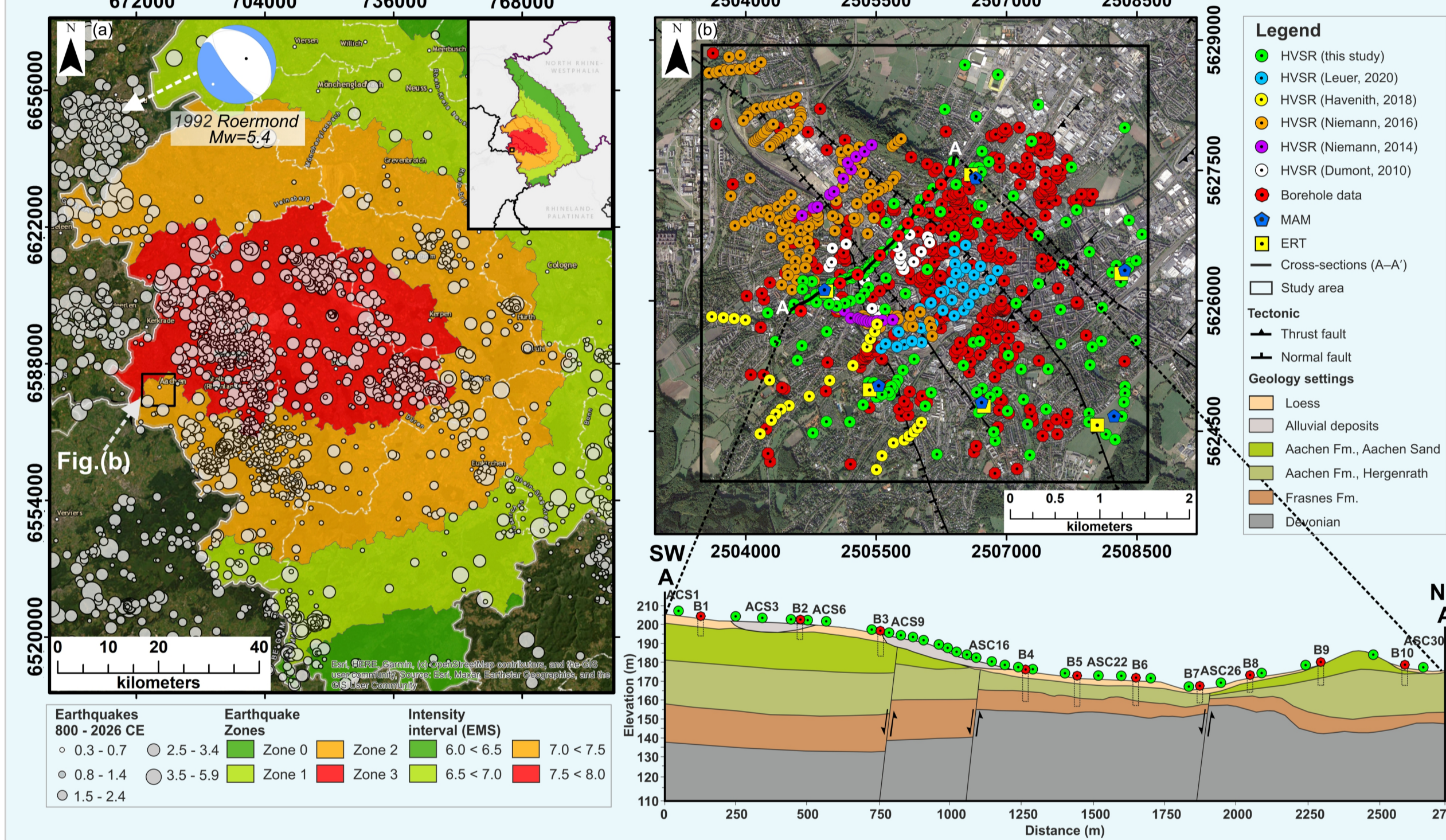
ASSESSMENT OF SEISMIC SITE EFFECTS IN AACHEN (GERMANY) TO SUPPORT SEISMIC MICROZONATION: GEOPHYSICAL OBSERVATIONS AND NUMERICAL MODELING

Farkhod Hakimov^{1,2}, Jochen Hürtgen¹, Hans-Balder Havenith², and Klaus Reicherter¹

¹ RWTH Aachen University, Neotectonics and Natural Hazards, Aachen, Germany
² University of Liège, Geology Department, Liège, Belgium

MOTIVATION & CONTEXT

Aachen, located in the Lower Rhine Graben, is exposed to moderate seismic hazard (EMS-98 VII–VIII; DIN 4149 Zones 2–3 [1–3]). The urban area is crossed by several NW–SE-trending normal faults — some of which are considered seismically active — that cause rapid lateral changes in soft sediment thickness across the entire city. However, the regional zonation considers entire zones as uniform, without differentiating local geology, fault geometry, or topography. The subsurface comprises Quaternary loess overlying Mesozoic clays and sands, disrupted by the active Laurensberg normal fault (25–35 m offset).



WHY IT MATTERS

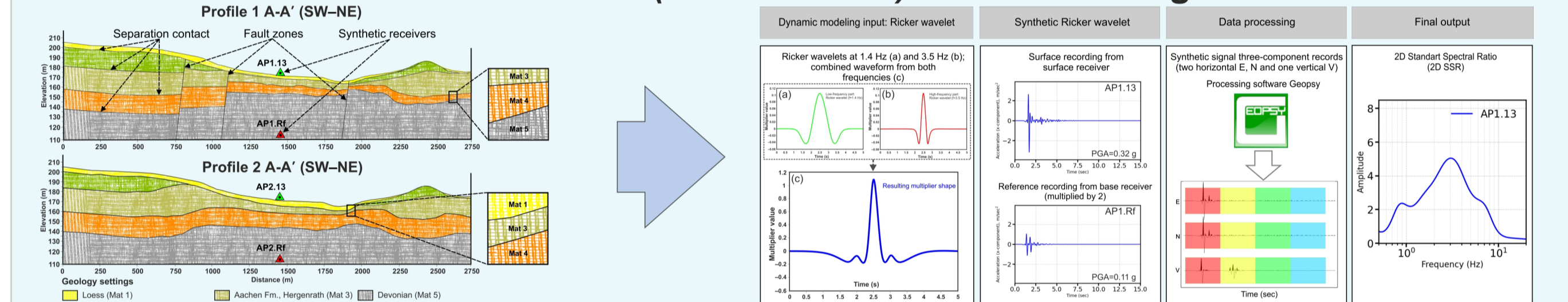
Site amplification effects can cause significant structural damage at considerable distances from earthquake epicentres, as demonstrated during the 1992 Roermond earthquake (Mw 5.4, ~50 km; [4]), when historic buildings in Aachen sustained damage at intensity VI (EMS-98). To quantify how local geology, faults, and topography shape the seismic response, we conducted a multidisciplinary geophysical campaign across a 5 × 5 km² area.

APPROACH

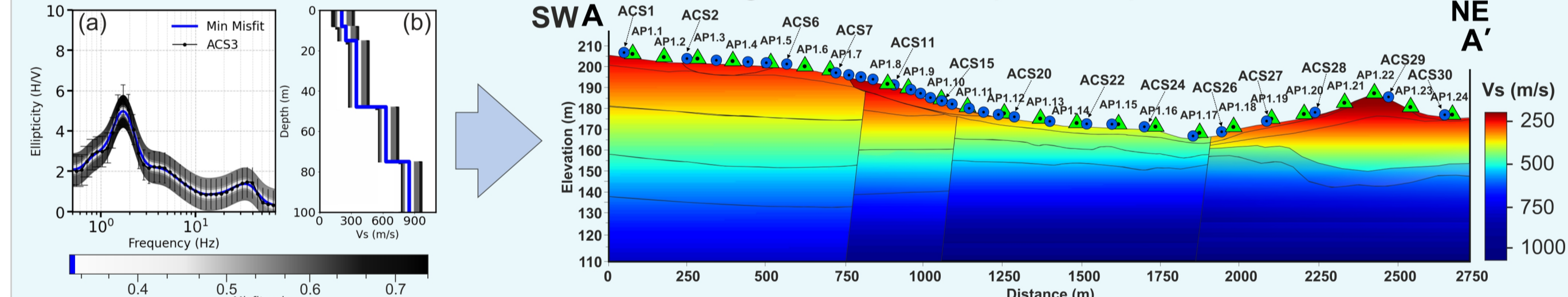
The investigation follows a four-stage workflow progressing from field observation to numerical prediction:

- Stage I — Mapping:** 475 single-station HVSr measurements (2010–2024) → f_0 , A_0 , and polarisation azimuth across the entire 5 × 5 km² study area.
- Stage II — Depth profiling:** Rayleigh-wave ellipticity inversion at 445 points and dispersion-curve analysis at six array measurements → provide V_s profiles. Six ERT profiles → stratigraphic control + fault detection. Constrained by 275 boreholes.
- Stage III — Numerical testing:** Two 2D dynamic models (UDEAC) along cross-section SW–NE: Profile 1 (with Laurensberg fault) vs Profile 2 (without). Dual Ricker wavelet input (1.4 + 3.5 Hz), 48 surface receivers.
- Stage IV — Validation:** 2D SSR curves compared with 30 HVSr measurements along cross-section SW–NE.

2D Numerical Models (Profiles 1 & 2) and Processing Workflow

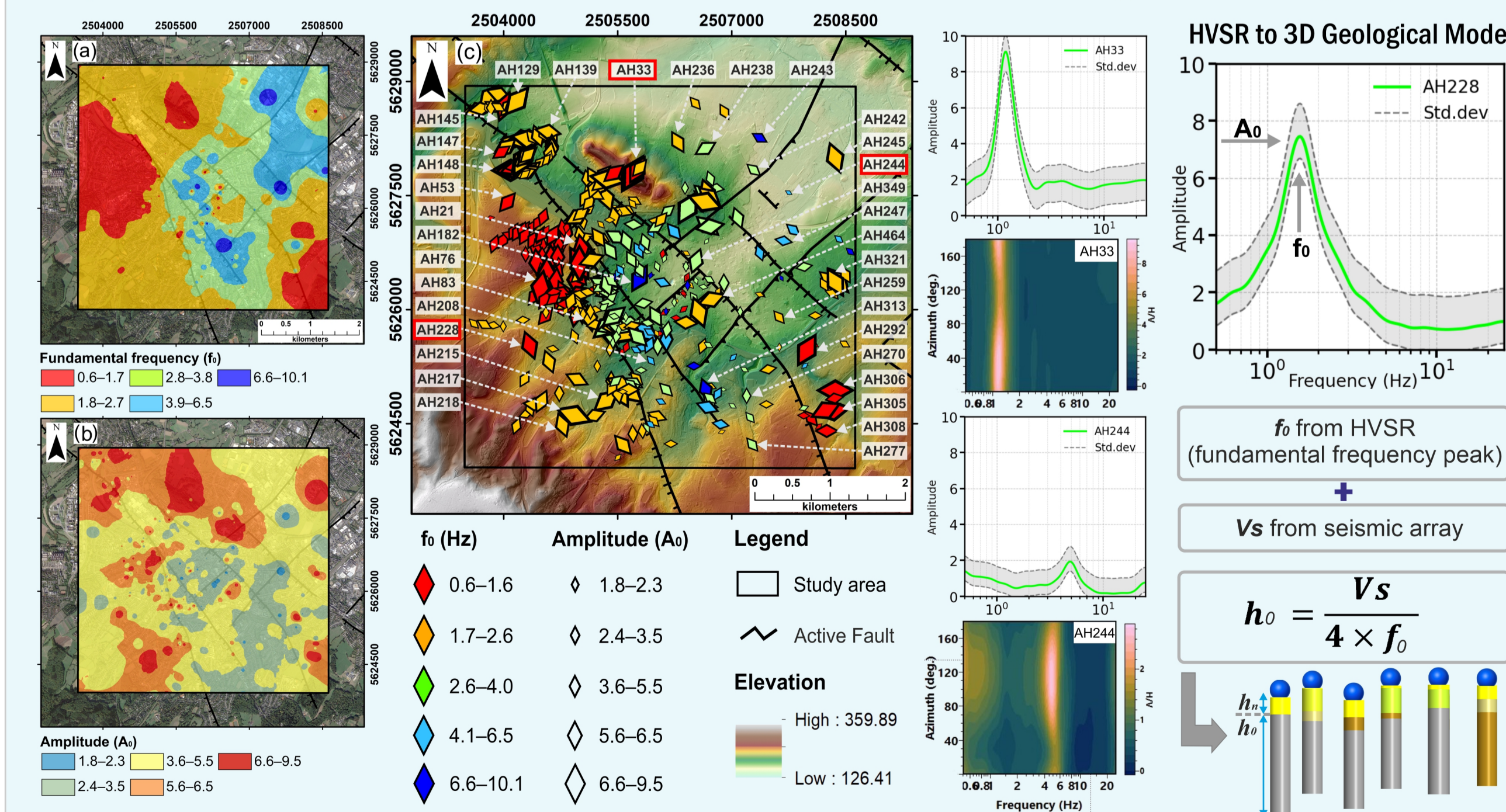


2D Vs Model along Profile A–A' (SW–NE)



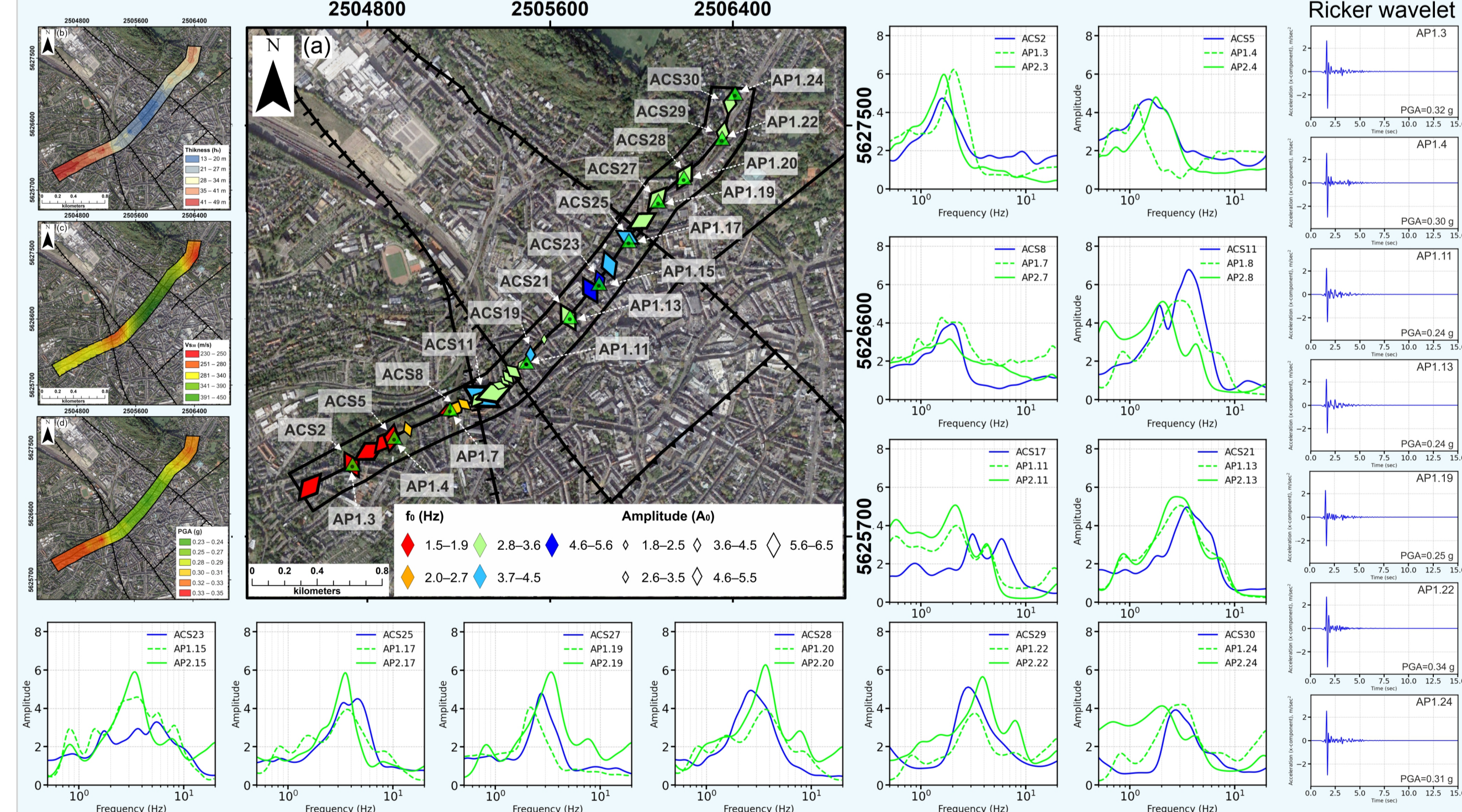
I. KEY FINDING: SPATIAL VARIABILITY OF SITE RESPONSE

Active normal faults cause rapid changes in sediment thickness, producing sharp site-response contrasts. W/NW/SW/SE: $f_0 = 0.6–2.6$ Hz, $A_0 = 3–8.5$, $V_{s30} = 230–340$ m/s [5]. Laurensberg hill: topographic amplification (~1 Hz). Central-east: minimal ($V_{s30} > 450$ m/s). HVSr polarisation subparallel to Laurensberg fault → waveguide effect [6, 7].



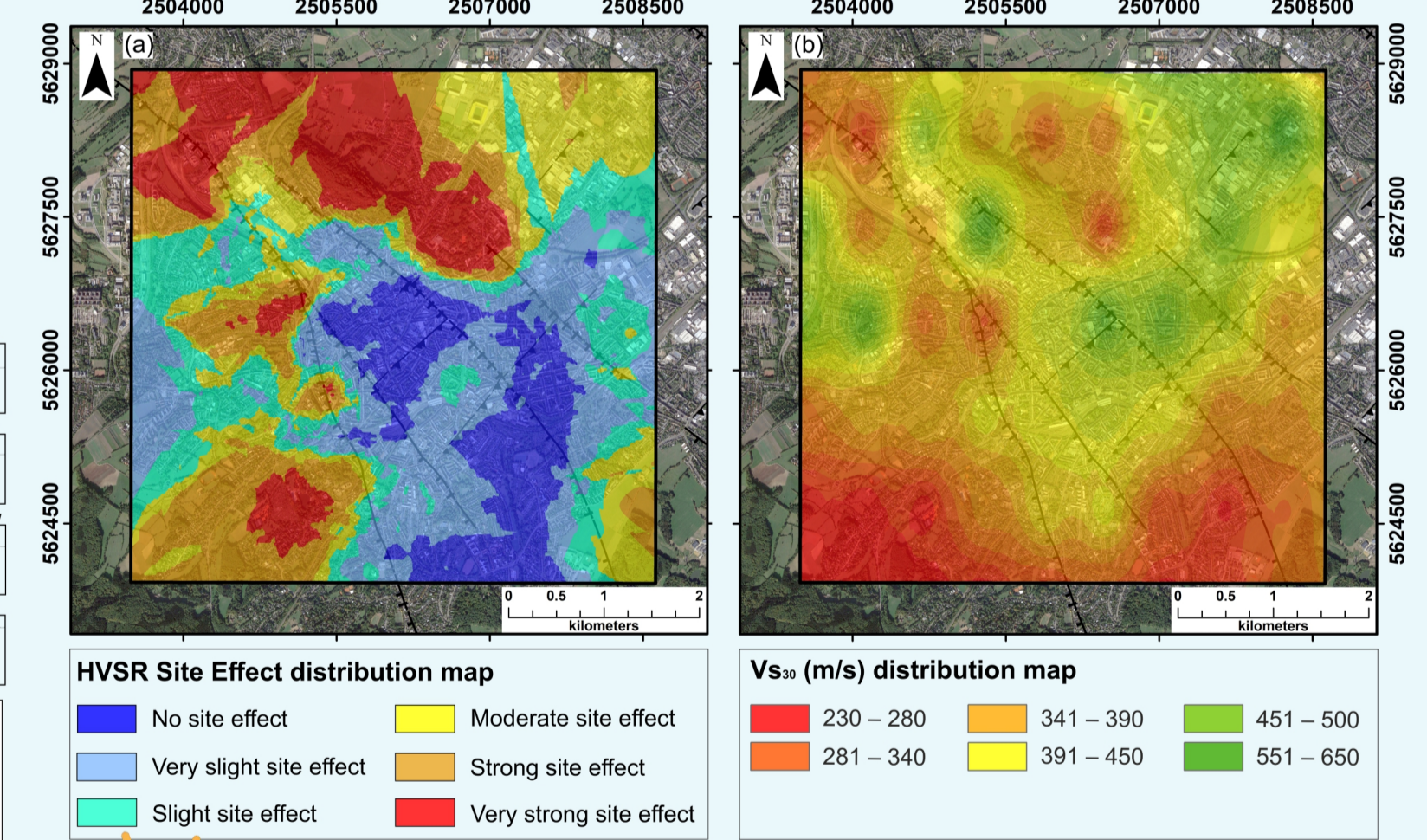
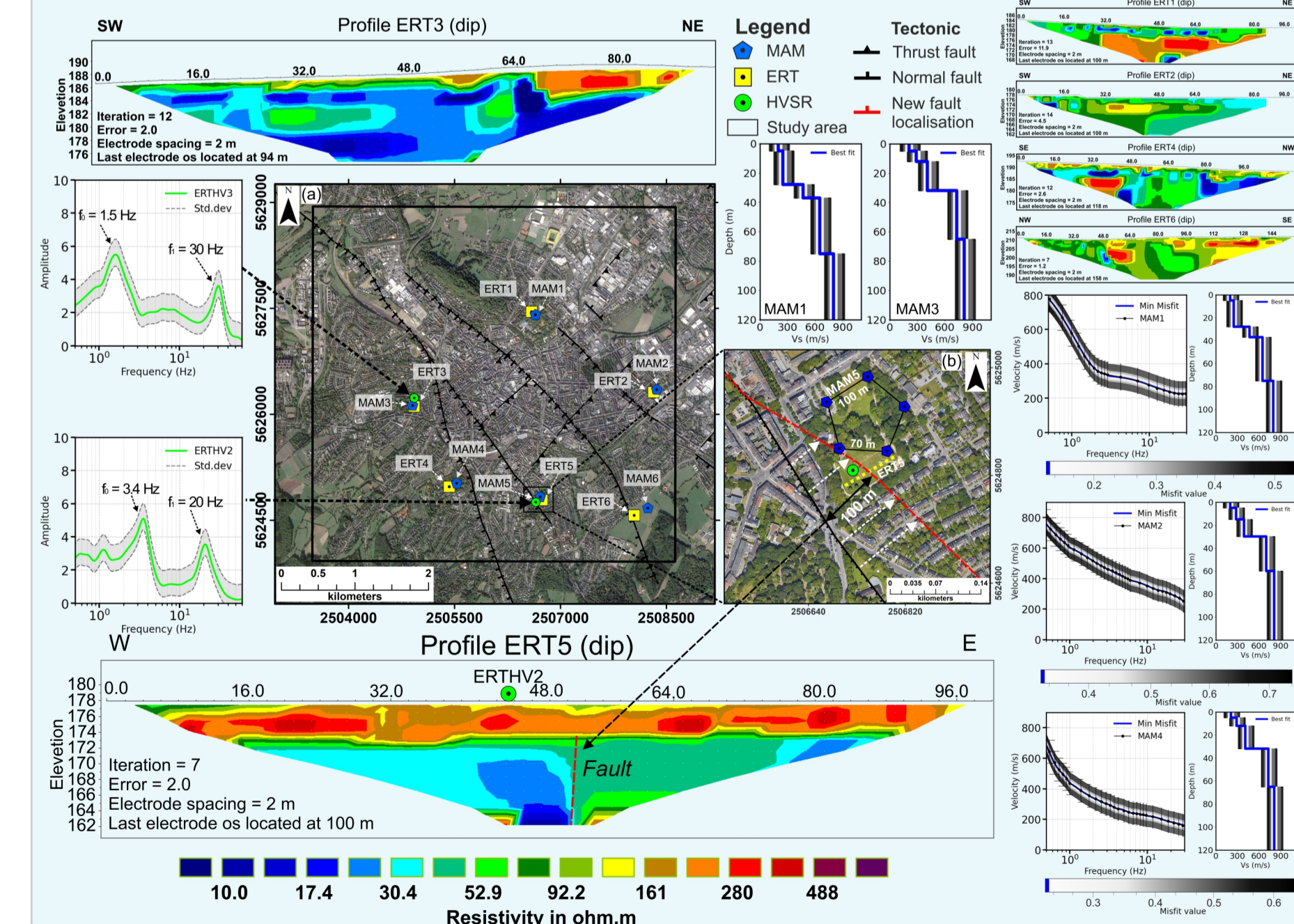
II. KEY FINDING: THE FAULT CHANGES EVERYTHING

ACS11 (20 m from fault): HVSr double peak at 1.9 + 3.7 Hz ($A_0 \approx 6.5$). Profile 1 (with fault) reproduces it; Profile 2 fails. PGA above fault: 0.28 g vs 0.39 g. Omitting fault → 11% PGA overestimation.



III. KEY FINDING: A HIDDEN FAULT REVEALED

ERT5 deployed across an approximately mapped fault. Three methods converge: (1) resistivity discontinuity (150–450 vs 30–50 Ω -m); (2) low V_s (280–380 m/s); (3) HVSr peak at 3.4 Hz ($A_0 \approx 6$). Fault relocated by several hundred metres.



TAKE-HOME MESSAGE

Within one DIN 4149 zone, PGA varies 0.23–0.35 g. Active normal faults redistribute seismic energy and control soft sediment thickness variations across the city. Topography amplifies it, Mesozoic sediments trap it. Regional zonation misses all three. *Site-specific microzonation is essential.*
Next: 3D modelling | ML classification | probabilistic hazard.

REFERENCES

- [1] DIN 4149:2005-04 (2005). Bauten in deutschen Erdbebengebieten — Lastannahmen, Bemessung und Ausführung ihrer Hochbauten. Deutsches Institut für Normung, Berlin.
- [2] Tyagunov, S., Grünthal, G., Wahlström, R., Stempniewski, L., Zschau, J., and Münich, J. V. (2006). Erdbebenrisiko-Kartierung für Deutschland. Beton- und Stahlbetonbau, 101(10), 769–782.
- [3] Müller, M., Vorogushyn, S., Maier, P., Thieken, A. H., Petrow, T., Kron, A., Büchele, B., and Wächter, J. (2006). CEDIM Risk Explorer – A map server solution in the project “Risk Map Germany”. Natural Hazards and Earth System Sciences, 6(5), 711–720.
- [4] Rolf Pelting. (1994). Source parameters of the 1992 Roermond earthquake, the Netherlands, and some of its aftershocks recorded at the stations of the Geological Survey of Northrhine-Westphalia. Netherlands Journal of Geosciences, 73, 215–223.
- [5] Hakimov, F., Havenith, H.-B., Ischuk, A., and Reicherter, K. (2024). Assessment of site effects and numerical modeling of seismic ground motion to support seismic microzonation of Dushanbe City, Tajikistan. Geosciences, 14(5), 117.
- [6] Di Giulio, G., Cara, F., Rovelli, A., Lombardo, G., and Rigano, R. (2009). Evidences for strong directional resonances in intensely deformed zones of the Perinca fault, Mount Etna, Italy. J. Geophys. Res., 114, B10308.
- [7] Pischiutta, M., Rovelli, A., Salvini, F., Fletcher, J. B., and Savage, M. K. (2023). Directional amplification at rock sites in fault damage zones. Appl. Sci., 13(10), 6060.

